New ADXD/EDXD Spectrometer for Determining the Structure of Melts at High Temperature

Sci. Rep. RITU A42 (1996) pp. 231-237
No. 1, March 1996

New ADXD/EDXD Spectrometer for Determining the Structure of Melts at High Temperature*

Kazumasa SUGIYAMA, Takeshi SHINKAI and Yoshio WASEDA
Institute for Advanced Materials Processing, Tohoku University, Sendai 980-77

(Received December 28, 1995)

A new spectrometer for angular dispersive X-ray diffraction (ADXD) and energy dispersive X-ray diffraction (EDXD) facility has been built using a vertical type $\theta-\theta$ goniometer, which makes possible to measure the diffraction profiles of high temperature melts over 200 nm^{-1}. The fundamentals of this facility were tested by obtaining the interference function of molten $NaAlSi_3O_8$ at 1460 K. The feasibility of the EDXD analysis for high temperature melts was also confirmed by obtaining the well resolved RDF of molten $LiNbO_3$ at 1550 K.

KEYWORDS: X-ray Diffraction, ADXD, EDXD, RDF, melt structure, high temperature

1. Introduction

There is an increasing demand for the understanding of various properties of oxide melts. As an example, physico-chemical properties of metallurgical slags (oxide mixture) is very important for discussing their role in slag-metal reactions. There have been a number of measurements of density, viscosity, surface tension and electrical conductivity of oxide melts. However, only a few investigations of the atomic structure analysis of molten oxides using the diffraction experiments have been reported, in comparison with their glassy state. X-rays, neutrons and electrons are frequently used to determine the structure of non-crystalline materials. Of course, X-ray diffraction is the most popular method for the structural analysis of liquids. The relation between observed intensity data and the radial distribution function (RDF) has been discussed in detail [1,2,3]. As for the form of the X-ray diffraction pattern for silicate melt samples is similar, the Faber-Ziman type interference functions $S(Q)$ [3,4] of the $Na_2Si_2O_5$ and $NaAlSi_3O_8$ melts by using Mo $K\alpha$ radiation are shown in Fig.1 together with that of Ga melt, as an example. Although all profiles consisting of a number of peaks are similar, the damping behavior of the intensity profiles of silicate melts are not monotonic in contrast to the Ga case. This is due to the difference in the fundamental features of atomic configuration between silicate melts and metallic melts and a distinct local nearest neighbor correlation such as SiO_4 and AlO_4 in silicate melts are known to produce this behavior.

One of the most important requirements in the structural analysis of oxide melts is to reveal the local ordering structure and its distribution, then the high resolution RDF will cover this problem. For this purpose, the energy dispersive X-ray diffraction (EDXD) method with white radiation may be one way, which makes it possible to obtain the structural information in wide Q-region. For instance, the interference function over the value of Q=200 nm^{-1} can be obtained when X-rays of E=40 keV with the scattering angle of 80° are used. This contrasts with the usual limit of 150 nm^{-1} obtained by the conventional angler dispersive X-ray diffraction (ADXD) method with Mo $K\alpha$ radiation. However, there are some unsolved problems in the EDXD analysis at the present time, such as the quantitative determination of the

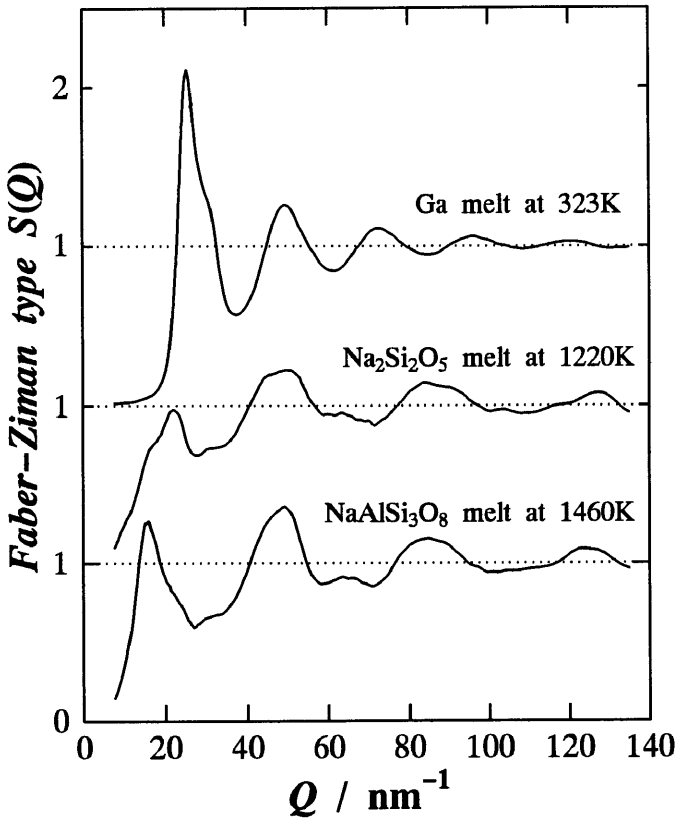

Fig.1 Faber-Zimen type interference functions $S(Q)$ for $Na_2Si_2O_5$ and $NaAlSi_3O_8$ melts, together with molten Ga.

* The 96-R2 report of Institute for Advanced Materials Processing (SOZAIKEN).

primary beam spectrum and a correction for Compton scattering. The relative advantage and disadvantage of the ADXD and EDXD methods have already been discussed in detail [4] and the difficulty in obtaining high resolution RDFs should be removed by simultaneous experiments of both methods. This strongly promotes us to make a new X-ray diffraction facility for making available the systematic ADXD/EDXD structure analysis of high temperature oxide melts using one spectrometer.

2. Fundamentals of the ADXD and EDXD method

An ordinary ADXD profile is measured using the characteristic X-ray radiations such as Cu $K\alpha$ and Mo $K\alpha$. The measurement up to 2θ=120° can cover a wave vector $Q=4\pi\sin\theta/\lambda$ region of 153 nm^{-1} in the case of Mo $K\alpha$, where 2θ and λ nm=1.24/E are the scatter-ing angle and wave length of X-ray, respectively. The observed scattering intensity $I^{obs}(Q)$ may be expressed by

$$I^{obs}(Q) = PAC[I^{coh}(Q)+I^{inc}(Q)] \quad (1)$$

where P is the polarization factor, A the absorption, C the geometric factor including the so-called normalization constant, and $I^{coh}(Q)$ and $I^{inc}(Q)$ are the coherent and incoherent scattering intensities in electron units per atom, respectively. In the ADXD analysis the factors P and A are dependent on scattering angle, the energy of X-ray and experimental conditions, and these are readily calculated from the analytical equations [4] and well compiled absorption coefficient data [5]. Therefore, the main purpose of the analysis is to obtain the quantity of $I^{coh}(Q)$ from the observed intensity. After the corrections of polarization and absorption, $I^{coh}(Q)$ in electron units per atom can be obtained by the generalized Krogh-Moe-Norman method [3,4]. This data processing includes the correction for Compton scattering [6,7,8] and Breit-Dirac recoil factor. It should be noted that the intensity of X-ray source $I_p(E)$ should be equal during each measure-ment and a constant value is used without any serious reservation in the ADXD analysis. The interference function $Qi(Q)=Q(S(Q)-1)$ can be obtained from the coherent intensities in the following form;

$$Qi(Q) = \frac{Q[I^{coh}(Q)-\langle f^2\rangle]}{\langle f\rangle^2} \quad (2)$$

where $\langle f\rangle$ is the average atomic scattering factor and $\langle f^2\rangle$ is the average square of atomic scattering factor [3,4]. By Fourier transformation of $Qi(Q)$, the ordinary RDF is readily calculated with the density value of the sample ρ_0;

$$4\pi r^2\rho(r) = 4\pi r^2\rho_0 + \frac{2r}{\pi}\int_0^\infty Qi(Q)\sin Qr\,dQ \quad (3)$$

On the other hand, the EDXD method using a solid-state detector (SSD) was recently applied to structural study of non-crystalline systems. The EDXD method utilizes white X-ray radiation and a fixed diffraction angle. This is a contrast with the conventional ADXD method, which uses a monochromatic X-ray and the angular scanning mode. Details of the principles and data analysis for the EDXD method for non-crystalline materials has been described as follows [9,10,11,12,13]. The intensity of the scattered X-rays can be given by;

$$I^{obs}(E,\theta)=C(E)[I^{coh}(E,\theta)+I^{inc}(E,E',\theta)] \quad (4)$$

$$I^{coh}(E,\theta)=A(E,E,\theta)P(E,E,\theta)I_p(E)I^{coh}(Q) \quad (5)$$

$$I^{inc}(E,E',\theta)= R(E,E')\left(\frac{dE'}{dE}\right)A(E,E',\theta)P(E,E',\theta)I_p(E')I^{inc}(Q') \quad (6)$$

where C is a normalization constant again, $I^{coh}(E,\theta)$ and $I^{inc}(E,E',\theta)$ are the coherent and incoherent scattering intensities at the scattering angle of 2θ, respectively. E' is the initial energy of the incoming X-ray photon which is reduced to E after the Compton scattering. $I_p(E)$ is the intensity profiles of the incoming X-rays. $P(E,E',\theta)$ and $A(E,E',\theta)$ the polarization and adsorption factor, respectively. The Breit-Dirac recoil factor $R(E,E')$ cancels out a correction factor of the incoherent spectrum contraction (dE'/dE), so that the product $(dE'/dE)R(E,E')$ becomes one for the EDXD analysis [9]. Analytical expression of the absorption factor $A(E,E',\theta)$ is applied with the mass absorption coefficient as a function of X-ray energies [14]. The polarization factor for white X-ray can be written as follows,

$$P(E,E',\theta)=\frac{1}{2}\left(\frac{E}{E'}+\frac{E'}{E}-\sin^2 2\theta\right)+\frac{1}{2}\pi(E)\sin^2 2\theta \quad (7)$$

where $\pi(E)$ is a degree of polarization of the incident X-rays defined by $(I_{pn}(E)-I_{pp}(E))/(I_{pn}(E)+I_{pp}(E))$, where $I_{pn}(E)$ and $I_{pp}(E)$ are the intensities of the normal and parallel polarization components as a function of the energy of X-rays, respectively. As an example, the factor of $\pi(E)$ for a W target at the accelerating voltage of 45, 50 and 60 kV was measured using the scattering intensity of SiO_2 glass [15] and the results are shown in Fig.2. The value of $\pi(E)$ is almost less than 0.1 below the X-ray energy of almost 75 % of the incident electron energy. Therefore, the polarization correction with respect to this factor has no significant effect on the EDXD analysis if only the energy region below about 75 % of the incident electron energy is applied.

$I^{coh}(Q)$ is the only structural dependent part of the total EDXD spectrum. In order to obtain $I^{coh}(Q)$, the most important data processing is the determination of the primary X-ray intensity $I_p(E)$, including the normalization

constant C. This can be readily done by using the X-ray scattering of the amorphous material itself. Since $I^{coh}(Q)$ will tend toward $\langle f^2 \rangle$ as the increment of Q, equation (4) can be reduced to the following expression in the large Q-region using $I_0(E)(=CI_p(E))$ [9,10,12].

$$I^{obs}(E,\theta)=I_0(E)\ [P(E,\theta)A(E,\theta)\langle f^2\rangle+ \frac{I_0(E')}{I_0(E)}P(E,E',\theta)A(E,E',\theta)I^{inc}(Q')] \quad (8)$$

Although the Compton shift becomes appreciable in the region with large values of E and 2θ, the assumption of $I_0(E)=I_0(E')$ is used in the first iteration step for obtaining the first order estimation of $I_{01}(E)$ from equation (8). In the second iteration step, the approximation of $I_0(E')/I_0(E)=I_{01}(E')/I_{01}(E)$ allows to obtain more reliable primary X-rays spectrum $I_{02}(E)$. Such calculating steps are continued with the approximation of $I_0(E')/I_0(E)=I_{0n-1}(E')/I_{0n-1}(E)$ where n is the iteration number. Four or five iterations are usually sufficient to ensure reliable $I_0(E)$, which enables us to explain measured intensity from the sample.

With thus estimated primary beam spectrum, it is now possible to calculate the Faber-Ziman type interference function $S(Q)$ in the limited Q-range from $I^{coh}(Q)$ at several fixed scattering angles as follows.

$$S(Q)=\frac{I^{coh}(Q)-[\langle f^2\rangle-\langle f\rangle^2]}{\langle f\rangle^2} \quad (9)$$

By combining different fragments of $S(Q)$, starting from the data for the 2θ run used to estimate the primary beam spectrum, the interference function in the wide Q-range can be obtained. From this full $S(Q)$ profiles, the high resolution RDF is readily calculated using the Fourier transformation of equation (3).

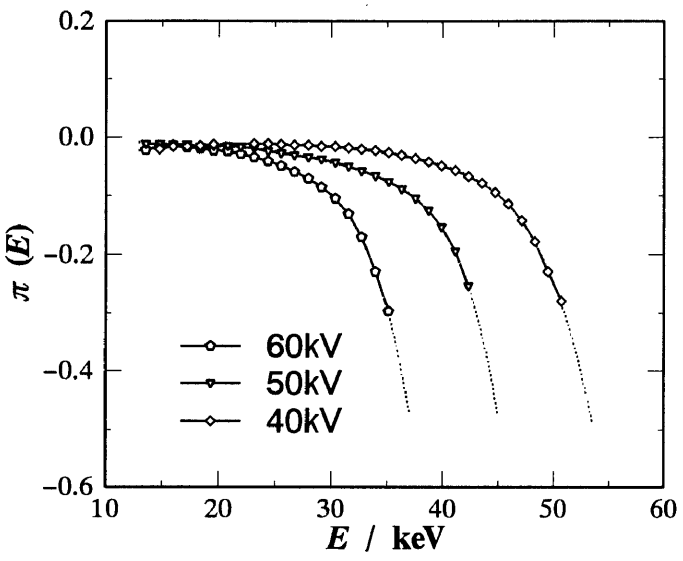

Fig.2 The measured polarization $\pi(E)$ for a W tube operated at 45, 50 and 60 KV.

3. Description of the ADXD/EDXD spectrometer

Figure 3(a) and (b) show the overall view, indicating the experimental setup of the present ADXD/EDXD facility in SOZAIKEN (Institute of AMP), respectively. This system consists of a $\theta-\theta$ type goniometer in the vertical setting where an X-ray tube and a detector can rotate in the opposite direction. This configuration makes it possible to measure the scattering intensities from the free surface of a melt sample. The high temperature chamber mounted in the center of a goniometer axis, has a slot with Be window (15 mm wide) through the water-cooled enclosure wall, allowing the passage of X-rays and controls the atmosphere around the melt samples. A sample cell is set on the heating block made of Al_2O_3 at the center of the chamber. This heater block is connected with the elevation and azimuth controls so that the melt surface of a sample cell can be set horizontal and at the same level with the goniometer axis. The wires of 0.8 mmϕ such as Mo, Pt-Ph or Kanthal are usually used as heating element and temperatures can be controlled within ±5 K by monitoring the output from the Pt-Pt13%Rh or W5%Re-W26%Re thermocouple just below the sample cell. It may be worth mentioning that the X-ray optics consists of three adjustable slits (divergent, receiving and scattering slits) with a pair of Soller silts. The width and height of the slits are adjusted so as to obtain a good compromise between counting rate and resolution in relevance to the scattering angle.

In the case of usual ADXD measurement, an X-ray tube with Mo anode (Rigaku A-41-Mo) operated with a constant potential generator (Rigaku 4037), is used to produce strong characteristic radiation. The scattering intensity is measured by an usual NaI(Tl) scintillation counter (SC) coupled with a pulse-height analyzer and a pyrolitic graphite monochromator in the diffracted beam path. The total intensity measured at the first peak of the scattering profiles is usually over 80000 counts, and at least 20000 counts are collected even at the angle of minimum intensity.

As for EDXD analysis, an X-ray tube with W (Rigaku A-41-W) is used to produce strong white radiation. The solid-state detector with intrinsic Ge (EG&G ORTEC GLP 16195/10P) is employed for the detection of scattering intensity spectrum. The signal from the pre-amplifier of SSD is delivered to a main amplifier (EG&G ORTEC 672) with a pile-up rejector. The shaping time is usually set to 6 μsec which offers a good compromise between high counting rate and resolution. A multichannel analyzer (Laboratory Equip. Co. MCA/98BX) is set to 1024 channels so as to cover the entire spectrum up to 60 keV (about 60 eV/channel). The relation of photon energy versus channel number was calibrated by measuring the fluorescent X-rays of several pure metals such as Fe, Mo and Pd. When X-ray photons come into the SSD, some portion of them is used to excite K core electrons of detecting materials of Ge. This causes the so-called escape effect by producing

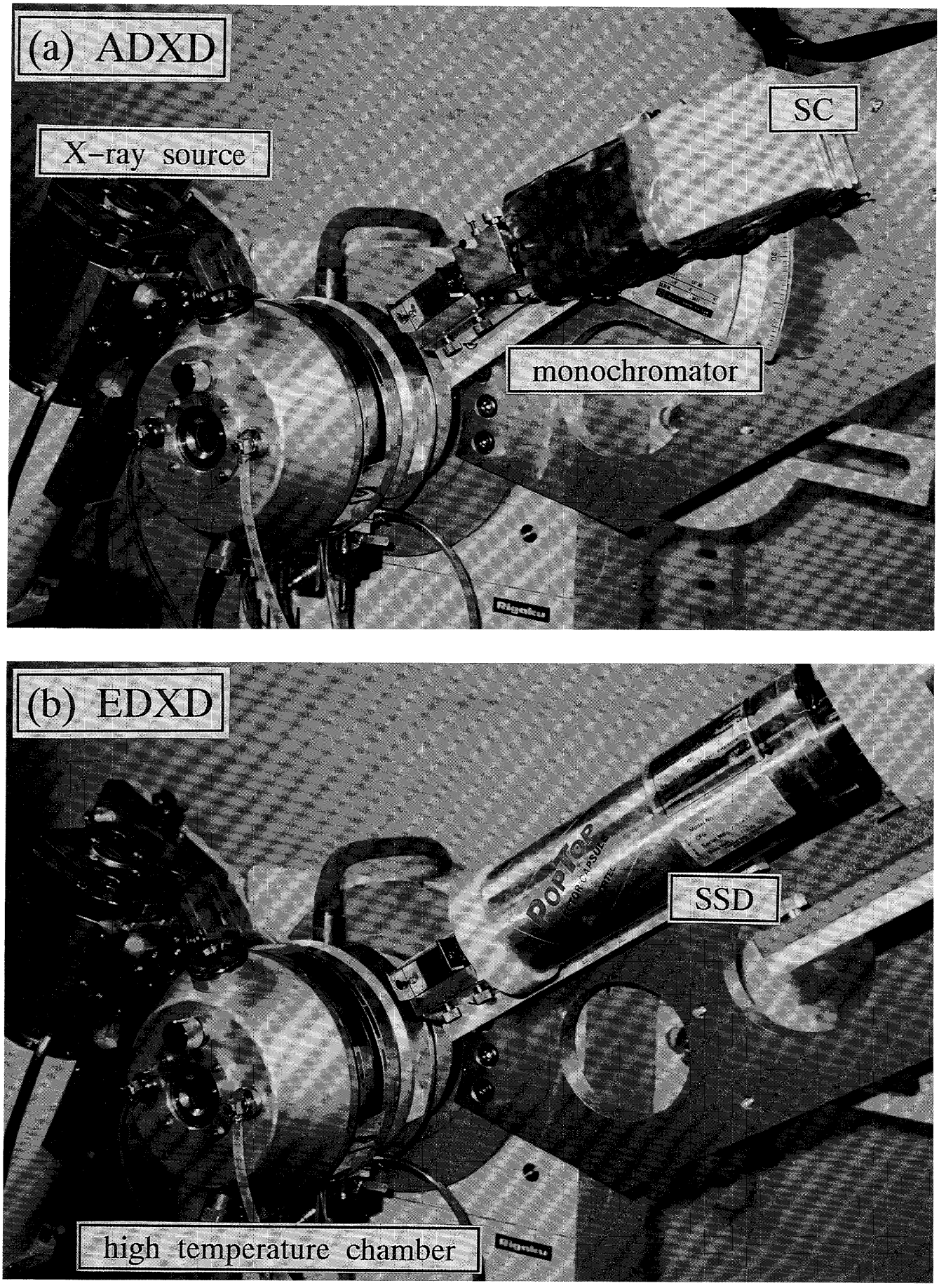

Fig.3 Overall view of present ADXD(a)/EDXD(b) spectrometer with a high temperature chamber for structural study of melts at SOZAIKEN (Institute of AMP).

a pair of peaks at positions where their differences are the energies of Ge $K\alpha$ and $K\beta$ radiations. The degree of this effect can be experimentally determined and is taken into account during EDXD data processing. The intensity over 30000 counts is always accumulated even at the channel of minimum intensity.

4. Structural analysis of high-temperature melts

The capability of the present ADXD/EDXD facility was tested by obtaining RDFs of $NaAlSi_3O_8$ and $LiNbO_3$ melts at 1460 K and 1550 K, respectively.

(1) $NaAlSi_3O_8$ melt

The $NaAlSi_3O_8$ glass sample is prepared from the chemical reagents of Na_2CO_3, SiO_2, and Al_2O_3 (Kanto Chemical Co.Ltd) and melted in a platinum cell (20x30 x3 mm^3) in air. The ADXD profiles was measured by Mo $K\alpha$ radiation with the operating conditions of 40 kV and 25 mA in the angular range from 2θ=6 to 100°, which corresponds the wave vector region of Q=6 to 135 nm^{-1}. The observed intensity data were analyzed through the common procedure described in the previous section, and the resultant $S(Q)$ data is given in Fig.1.

In the EDXD analysis, the determination of the whole part of $S(Q)$ requires several segments at different 2θ angles. The angular settings have to be chosen in such a way that any two consecutive 2θ angle runs overlap in the sufficient range in Q-space. The white X-rays were generated by a W tube with the operating conditions of 55 kV and 20 mA. The diffraction spectrum were measured at 2θ=6, 8, 15, 20, 38, 48, 60 and 74°. Through the data processing of EDXD, the calculated segments of $S(Q)$ in the $NaAlSi_3O_8$ melt were jointed so as to obtain full $S(Q)$ profiles as shown in Fig.4. The resultant $Q(S(Q)-1)$ and RDF of the $NaAlSi_3O_8$ melt at 1460 K are given in Fig.5 and Fig.6, respectively.

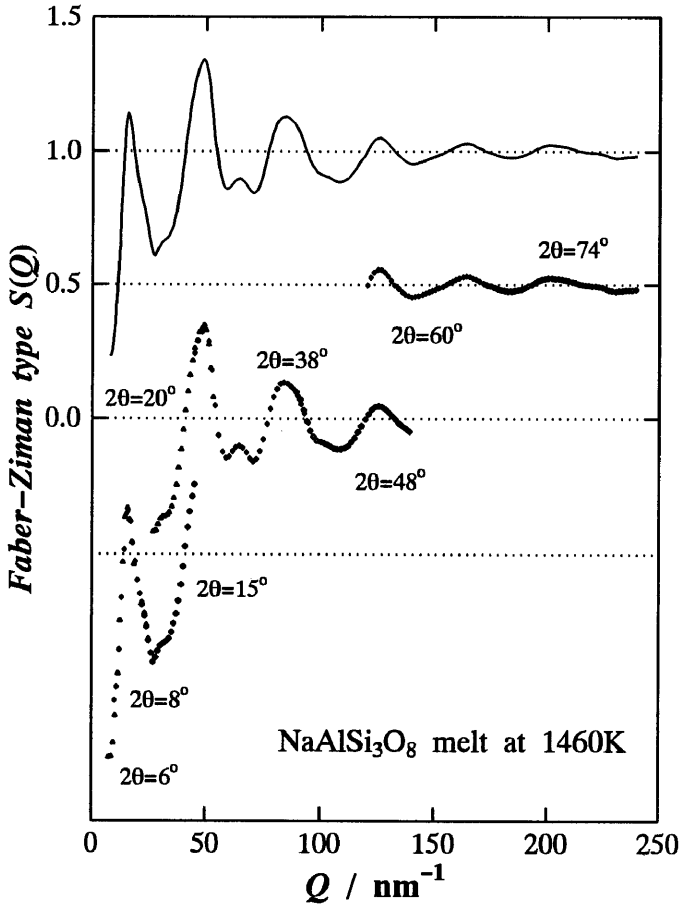

Fig.4 The obtained fragments of $S(Q)$ of $NaAlSi_3O_8$ melt at 1460 K.

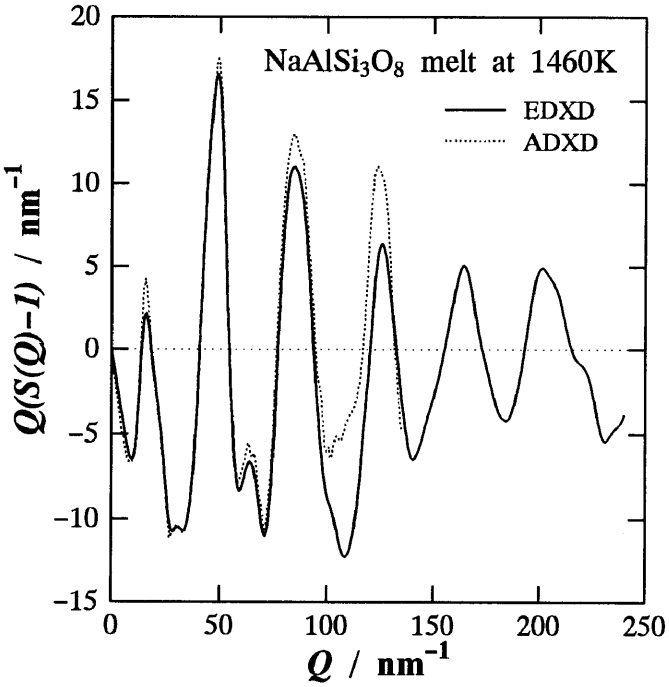

Fig.5 $Q(S(Q)-1)$ functions of $NaAlSi_3O_8$ melt at 1460 K. The solid line denotes the EDXD data, and dotted line is the result of ADXD.

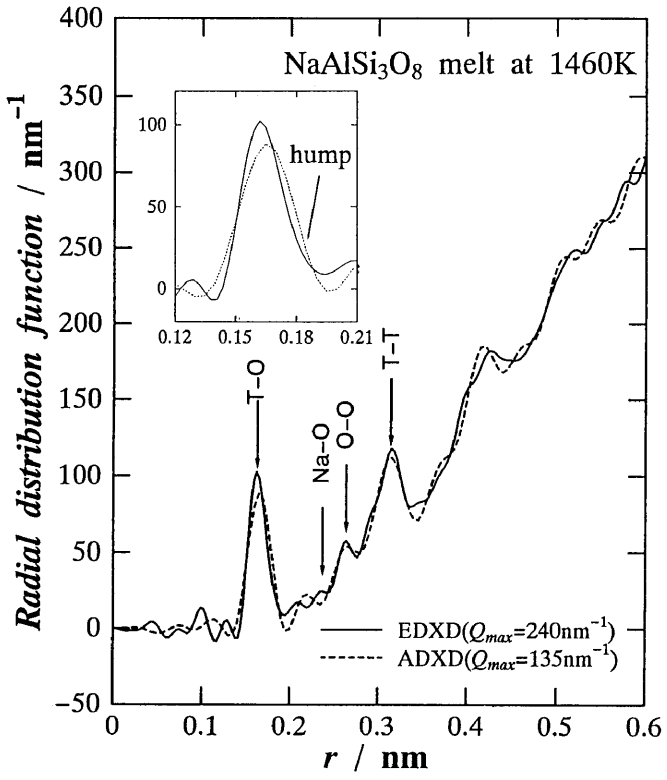

Fig.6 RDFs of $NaAlSi_3O_8$ melt at 1460 K. The solid line is the EDXD result, and dotted line is the ADXD result. The arrows indicate positions of some atomic pairs observed in crystalline $NaAlSi_3O_8$. (T = Si and Al)

Both structural functions of $NaAlSi_3O_8$ melt determined by the ADXD and EDXD method are found to agree well with each other. It is rather stressed here that the present RDF data of EDXD is superior to that of ADXD in its resolution because the interference function is determined in the wide Q-region up to 240 nm^{-1}. In particular, the contribution of Si-O (0.161 nm) and Al-O (0.173 nm) atomic pairs are likely to be separated by showing the small hump at the long r side of the first peak of about 0.16 nm. This may reflect the difference in SiO_4 and AlO_4 tetrahedra in the melt structure. These result clearly indicates that the present ADXD/EDXD facility basically works well on structural investigation for oxide melt samples.

(2) $LiNbO_3$ melt

A large amount of oxide single crystals are known to be produced from the melts using Czochralski method. $LiNbO_3$ crystal is classified into this category and is expected to be widely applied as optical devices because of its excellent electro-optical properties. The measurements of physical properties of $LiNbO_3$ melts indicated anomalous behavior [16] and this is suggested to cause the certain local fluctuations of refractive index and light scattering center. Therefore, the structural information of the high temperature melt is strongly required for up-grading the quality and scaling up the single crystal size. New EDXD facility has been applied to the investigation for this $LiNbO_3$ melt. Single crystal flakes of $LiNbO_3$, provided by Mitsui Mining and Smeltting Co. Ltd., were charged into a Pt container (20x30x3 mm^3) and melted at 1550 K in air. The white X-rays were generated by a W tube with the operating conditions of 60 kV and 35 mA. The diffraction spectrum were measured at 2θ=6, 8, 10, 15, 20, 30, 40, 60 and 75°. It should be worth mentioning that the combination of Al plate (300 μm) and Cu foil (30 μm) was applied as a X-ray filter so as to reduce the strong fluorescence radiations of Nb $K\alpha$ and $K\beta$ in the measured EDXD spectrum. Figure 7 shows the resultant RDF of $LiNbO_3$ melt, together with that obtained by the ADXD measurement [17]. In this figure, the arrows indicating some atomic pairs in the crystalline $LiNbO_3$. From the present EDXD result, we can find the useful information concerning the melt structure of $LiNbO_3$.

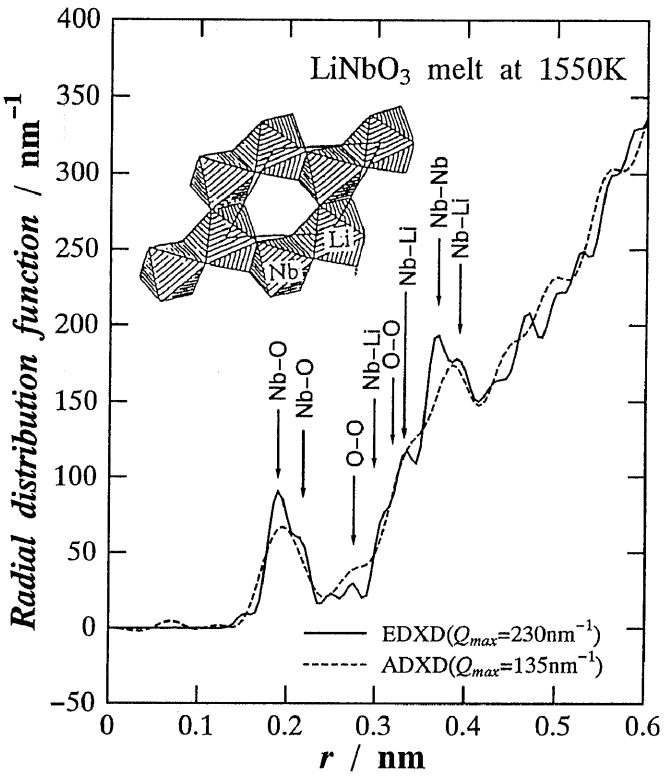

Fig.7 RDFs of $LiNbO_3$ melt at 1550 K. The solid line is the present EDXD result, and dotted line is the ADXD result [17]. The arrows indicate positions of some atomic pairs observed in crystalline $LiNbO_3$.

Figure 7 clearly indicates that the interference function with the wide wave vector region is very effective in order to obtain the high resolution RDF. This is particularly seen in the profiles of first neighboring Nb-O pair at about 0.20 nm. The local ordering unit of the melt is the octahedrally coordinated NbO_6. The first peak with small hump for the nearest neighbor Nb-O atomic pairs apparently indicates that a strong repulsion of cation-cation configuration is still realized even in the melt structure at high temperature. The rather broad distribution of cation-cation atomic pair in the distance from 0.3 to 0.4 nm implies the disordered distribution of Nb atom, along the way similar to the structures of α-Al_2O_3. These features may be attributed to the formation of relatively large clusters composed of NbO_6 octahedra, which is different from those of crystalline state. A detailed structural model of $LiNbO_3$ melt is outside of the scope of present paper. Nevertheless, the present authors would suggest that new ADXD/EDXD facility is suitable enough to obtain the high resolution RDFs of oxide melts by making available the interference functions in wide wave vector region.

5. Concluding remarks

The high temperature angular dispersive X-ray diffraction(ADXD) and energy dispersive X-ray diffraction (EDXD) facility has been newly developed, which is equipped with a vertical type $\theta-\theta$ goniometer and a high temperature chamber. This arrangement is very useful for measuring the scattering intensities from the free surface of the molten samples. The capability of this ADXD/EDXD apparatus was well-demonstrated by obtaining the reduced interference functions of the molten $NaAlSi_3O_8$. The structural analysis for the molten $LiNbO_3$ has also been carried out using the present facility. The obtained interference function over 200 nm^{-1} and its corresponding high resolution RDFs clearly indicate that the EDXD method is one of the powerful tools for structural characterization of various oxide melts at high temperature.

Acknowledgements

This work was carried out as part of a research project, financially supported by a Grant-in-Aid for Scientific Research (B) (No.06452308) from the Ministry of Education, Science and Culture of Japan. The authors wish to thank Dr.S.Kimura of National Institute for Research in Inorganic Materials for his kind advice.

1) H.P.Klug and A.E.Alexander: *X-ray Diffraction Procedures*, John Wiley & Sons, Inc., New York (1954).
2) B.E.Warren: *X-ray Diffraction*, Addison-Wesley, New York(1969).
3) C.N.J.Wagner,H.Ocken and M.L.Joshi: Z.Naturforsch.**20a**(1965)325.
4) Y.Waseda: *The Structure of Non-crystalline Materials*, McGraw-Hill, New York(1980).
5) *International Tables for X-ray Crystallography* Vol.IV, The Kynoch Press, Birmingham(1974).
6) D.T.Cromer and J.B.Mann: J.Chem.Phy.**47**(1967)1892.
7) D.T.Cromer: J.Chem.Phy.,**50**(1969)4857.
8) V.H.Smith Jr,A.J.Thakkar and D.C.Chapman: Acta Cryst.,**A31**(1975)391.
9) T.Egami: J.Mater.Sci.,**13**(1978)2587.
10) C.N.J.Wagner, D.Lee, S.Tai and L.Keller: Advancesin X-ray Analysis,**24**(1981)245.
11) R.Utz, A.Brunsch, P.Lamparter and S.Steeb: Z.Naturforsch.**44a**(1989)1201.
12) J.M.Prober and J.M.Schultz: J.Appl.Cryst.,**8**(1975)405.
13) K.Nishikawa and T.Iijima: Bull.Chem.Soc.Jpn.**57**(1984)1750.
14) Y.Waseda: *Novel Application of Anomalous X-ray scattering for structural characterization of disordered Materials*, Springer-Verlag, New York(1984).
15) J.S.Olsen, B.Burass, T.Jensen, O.Alstrup, L.Gerward and B.Selsmark : Acta Cryst.**A34**(1978)817.
16) K.Shigematsu, Y.Anzai, S.Morita, M.Yamada and H.Yokoyama: Jpn J.Appl.Phys.**26**(1987)1988.
17) K.Sugiyama, K.Nomura, Y.Waseda, P.Andonov, S.Kimura and K.Shigematsu: Z.Naturforsch.**45a** (1990)1325.